Removal of VOCs from indoor environment by ozonation over different porous materials

C.W. Kwong, Christopher Y.H. Chao[*], K.S. Hui, M.P. Wan

Department of Mechanical Engineering, The Hong Kong University of Science and Technology, Clear Water Bay, Hong Kong

Abstract

Ozonation of toluene over NaX, NaY and MCM-41 adsorbents was studied targeting for indoor air purification. The combined use of ozone and the various micro- or meso-porous adsorbents aimed to take advantage of the strong oxidizing capability of ozone. At the same time the residual ozone would be minimized due to the enhanced catalytic reaction in the porous structure. To lower the residual ozone level is a crucial issue as ozone is itself an indoor pollutant. The Lewis acid sites in the adsorbents were believed to decompose ozone into atomic oxygen, and the subsequent reactions would then convert the adsorbed toluene into CO_2 and H_2O. In the dry conditions, the MCM-41 required the smallest amount of material to achieve the 90% reduction target, followed by NaY and NaX. In the more humid environment (50% RH), extra amounts of MCM-41 and NaX adsorbents were required to reach the target as compared with the dry conditions. Desorption experiments were also conducted to study the amounts of various major species held in the adsorbents during the catalytic process. A material balance analysis of the major species in both the effluents and the adsorbents showed that within our experimental conditions, about 20–40% of the removed toluene was carried out via catalytic ozonation while adsorption covered the rest. Trace amount of intermediate species such as aldehydes and organic acids were identified in the desorbed gas indicating that they were withheld by the adsorbents during the air purification process and those in the effluent were below detection levels.
© 2007 Elsevier Ltd. All rights reserved.

Keywords: Ozone; VOC; Toluene; Zeolite; Adsorbent

1. Introduction

Uses of porous materials such as activated carbon or zeolite are well-established methods to control indoor volatile organic compounds (VOCs). These materials possess large surface area with high adsorption capacity and are frequently employed in traditional air purification systems (Chandak and Lin, 1998; Delage et al., 2000). Activated carbon offers a cost-effective way to minimize the pollutant level, while meso-porous molecular sieve MCM-41 shows promise as a potential adsorbent for VOC removal at high humidity level due to its high selectivity (Zhao et al., 1998). However, these adsorption techniques only transfer the containments to another phase. In recent years, some researchers employed ultra-violet photocatalytic oxidation (UV-PCO) techniques to eliminate VOCs (Yang et al., 2007). Several studies (Yu et al., 2006; Zhang et al., 2003; Hodgson et al., 2007)

*Corresponding author. Tel.: +852 2358 7210; fax: +852 2358 1543.

E-mail address: meyhchao@ust.hk (C.Y.H. Chao).

demonstrated the potential applications of UV-PCO reactors in indoor environments. However, emissions of intermediates (Sæbjörnsson and Fang, 2006) and UV lamp operation costs may be concerns.

In addition to these air purification technologies, ozone was also used as a cleaning agent in some air purifiers to remove VOCs (Yu et al., 2005; Boeniger, 1995). However, the VOC removal efficiencies by ozone alone were low and certain harmful by-products could be produced (USEPA, 2007). Reactions between excessive residual ozone (Niu et al., 2001) and unsaturated VOCs containing unsaturated carbon–carbon bonds may lead to the formation of harmful intermediate such as aldehydes, organic acids and fine mode particles (Weschler, 2000). The reaction rates of ozone with most VOCs were slow in indoor environments because the characteristic residence times of air and pollutant mixtures in typical indoor settings were too short for the reactions to proceed effectively (Weschler, 2000). Chen et al. (2005) evaluated several air cleaners in the indoor environment and found VOC removal efficiencies by ozone based air purifiers low and the indoor ozone could be at unsafe levels.

Despite the various issues in using ozone as a cleaning agent and the limitations in using adsorption techniques to adsorb VOCs, ozone has a very strong oxidizing capability and many zeolite or related porous materials may act as a catalyst when such a strong oxidizer is available, due to their ion exchange and other chemical features. Catalytic reactions normally occur at temperatures higher than room air temperature due to the high activation energy involved. If ozone is coupled with a suitable adsorbent to treat the indoor pollutants, the overall conversion efficiency may be increased even at room temperature, while maintaining the residual ozone level low. In addition, the energy consumption in using such a system may be minimized since frequent regeneration and intensive energy supply may not be required.

Several researchers (Oyama, 2000; Kastner et al., 2005; Einaga and Futamura, 2004) demonstrated the gas-phase catalytic ozonation of air pollutants in different systems. One study employed recycled material as an adsorbent, coupled with ozone for gas-phase catalytic ozonation of high volume low concentration sulfur compound emissions (Kastner et al., 2005). High conversion efficiency was achieved at room temperature. Einaga and Futa-

mura (2004) examined the catalytic oxidation of benzene with ozone over alumina-supported manganese oxides. They noticed that manganese oxides would effectively decompose ozone into atomic oxygen and reacted with benzene. The gas-phase ozonation of air pollutants has been studied in the past but not much information was obtained regarding the ozonation effects over molecular sieves and the basic mechanisms involved. Our previous findings indicated that ozone could be coupled with zeolite to achieve better VOC removal (Law et al., 2004; Chao et al., 2007). Results showed that the toluene conversion could be improved compared to using ozone or the adsorbent alone (Chao et al., 2007). Ozone can be decomposed into atomic oxygen in the Lewis acid sites of zeolite and subsequently reacts with toluene to form CO_2 and H_2O. The residual ozone and the reaction by-products could be kept at rather low levels. Our results also showed the adsorption capacity and acid strength of NaX limited the oxidation performance of toluene, with the zeolite deactivated in a few hours due to adsorption of water. This study aimed to explore the performance of some alternative adsorbents with higher adsorption capacity and stronger acidity compared to NaX.

NaY and MCM-41 were explored in this study. NaY is a hydrophobic zeolite and is not significantly affected by moisture while its catalytic properties are similar to that of NaX. The MCM-41 adsorbent has high surface area and stronger acid strength. Toluene is commonly found in indoor environments, from painting to other consumer products such as hair spray. The inlet toluene concentration was fixed at 1.5 ppm in this study for most experiments as this was the odour threshold level. This concentration level may not be easily recognized and may increase the health risk during long term exposure (OSHA, 2007). Toluene concentration of 0.3 ppm was also tried in a few cases to see the effect of low VOC level.

2. Experimental

2.1. Materials

Zeolite NaX and NaY were obtained commercially (Sigma-Aldrich) in powder form with 2 μm average particle sizes. The MCM-41 adsorbent with 0.1 μm particle size was synthesized following the procedures by Hui and Chao (2006) with different silica and aluminium sources. Sodium silicate

(Fisher Chemical) was used as the silica source and aluminium nitrate (Nacalai Tesque) was used as the post-synthesis aluminium source (Ryoo et al., 1997).

2.2. Methodology

The schematic diagram of the fixed-bed flow reactor for the experiments is shown in Fig. 1. Both adsorption and desorption experiments on the porous materials were conducted in the same reactor. The reactor had three sections: the inlet, the test and the sampling sections. The inlet section consisted of the supply gas system for the controlled experimental conditions. Toluene was supplied by standard toluene gas cylinder with 5 ppm toluene in N_2. The toluene gas standard was mixed and diluted with synthetic air with the toluene level in the inlet section adjusted by the mass flow ratio between the synthetic air and the standard toluene gas.

Ozone was generated by corona discharge from two ozone generators (Telewin, Model: Q(FCL)GF005-92). A 50 L stainless steel reservoir with fan mixers was used as a concentration stabilizer. The concentration of ozone in the inlet

section was controlled by the ozone generation rate and the mass flow rate through the reservoir to the test section. The gases were mixed with a mixer before entering the test section. This section consisted of a 700 W infrared heater, a temperature controller, a thermocouple, thermal insulation materials, stainless steel/quartz tube with 7 mm ID, bed-length selection valves and the adsorbents. The temperature of the test section was controlled by the temperature controller (Cole Parmer Digi Sense, Model: 89000-05) with a K-type thermocouple installed. The temperature could vary from ambient to 500 °C (± 1 °C). Three quartz tubes of 7 mm ID and 150 mm length each were connected in series. The adsorbents were put in the quartz tubes, with bed length ranging from 150 to 450 mm and an absorbent mass of approximately 2–5 g. The quartz tube was covered with Kaowool material to minimize heat loss and stabilize the reactor temperature.

The adsorption experiments were conducted at ambient temperature (25 °C), while the thermal desorption experiments were conducted at 350 °C. The sampling section consisted of four sampling ports located at the upstream and the downstream

Inlet section
1. Toluene gas
2. Synthetic air
3. Ozone generators with stabilizer
4. Flow controllers
5. Mixer

Test section
6. Adsorbents
7. Temperature controller
8. Bed-length selection valve
9. Kaowool thermal insulation

Sampling section
10. N_2 purge valve
11. N_2 gas
12. Photoacoustic multi-gas monitor
13. Ozone monitor
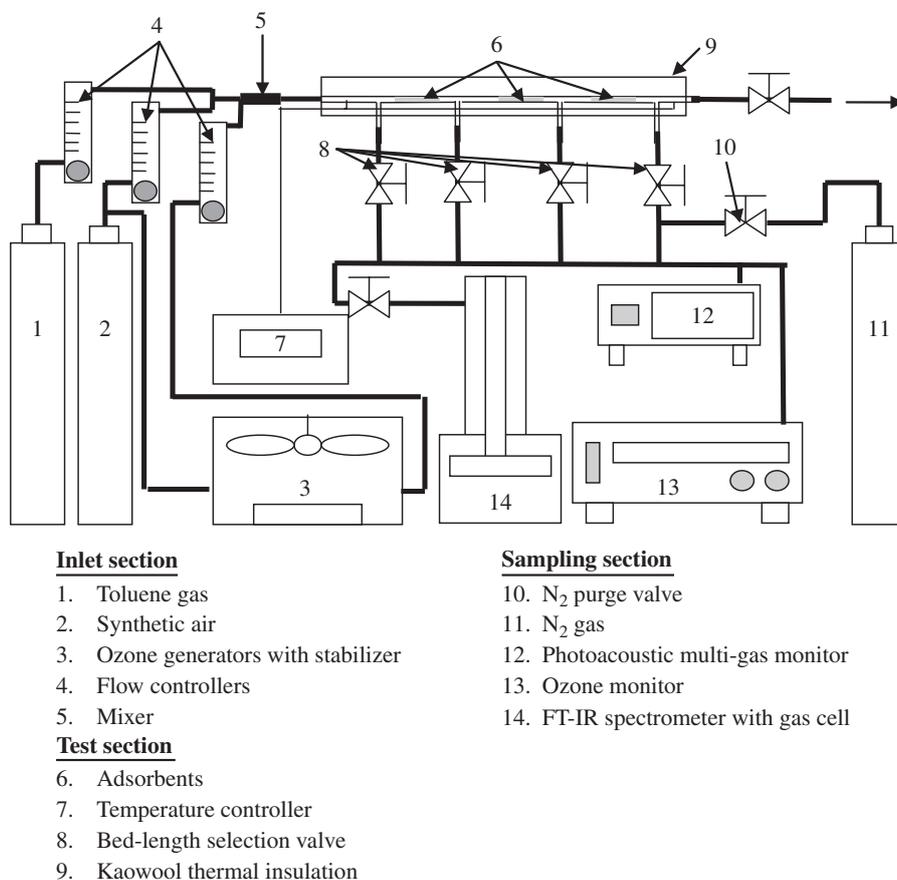14. FT-IR spectrometer with gas cell

Fig. 1. A schematic diagram of the testing facility.

positions of the quartz tube. Valves were installed so that upstream and downstream samples at various adsorbent bed lengths could be analysed. N_2 was purged to the sampling pipes at the beginning of each experiment to minimize the influence of the residual gases from last set of experiment.

2.3. Instruments and procedures

The ozone concentration was monitored by an ozone monitor (API Ozone monitor, Model: 450) based on absorption of 245 nm UV light. Real-time RH level, CO_2 and toluene concentration were measured using a photoacoustic multi-gas monitor (Innova, Model: 1312). The measurement principle is based on the photoacoustic infrared detection method, with detection limit for RH, CO_2 and toluene of 50, 3.4 and 0.04 ppm, respectively. The internal water vapour and CO_2 compensation algorithms in the gas monitor were enabled to minimize the cross interference. The monitor was calibrated with standard toluene gas in the range of 50–3000 ppb at 0% RH and 0% CO_2 levels. Linear plots of known toluene concentration against the signal strength obtained from the gas monitor were used for calibration. The flow rate of gas from the cylinders to the inlet section was controlled by flow controllers. The RH, CO_2, toluene and O_3 level were monitored both at the upstream and downstream positions of the test section. Apart from those regular species, the intermediate species of the gas stream were identified by the gas phase FT-IR spectrometer (Bruker, Model: Tenser 27) equipped with gas cell (Infrared Analysis, Model: 35-V-H) of 35 m path length.

The adsorbents were identified by powdered X-ray diffraction (PXRD) (Philips, Model: PW1830) and energy dispersive analysis using X-ray spectrometry (EDAX) (JEOL, Model: JSM 6300). The databases in the Joint Committee on Powder Diffraction Standards (JCPDS) were used to verify the crystal structure and the phase purity. The bulk chemical composition of the zeolite was measured by the X-ray fluorescence spectroscopy (XRF) (JEOL, Model: JSX-3210Z) element analyser for non-destructive quantitative and qualitative analyses.

Pore surface area of zeolite was determined by using a Brunauer Emmett Teller (BET) surface area analyser (Coulter, Model: SA3100) with nitrogen as the adsorbate. The sample surface areas were determined by physical adsorption of nitrogen at

$-196\,^{\circ}C$. The samples were outgassed at $250\,^{\circ}C$ for 2 h prior to the nitrogen adsorption–desorption experiments. Specific surface area was calculated from BET-isotherm.

The NH_3-TGA method was used to compare the acid site density and acid strength of the adsorbents. The adsorbents were allowed to adsorb the saturated ammonia vapour from the ammonium hydroxide solution (Fisher Scientific) for 30 min. The treated sample of 16 mg was then put into the TG/DTA analyser (Setaram, Model: TG-DTA 92-16). The sample was heated from 25 to $400\,^{\circ}C$ at the rate of $5\,^{\circ}C\,min^{-1}$ in N_2. The weight changes of the samples were plotted against the temperature and the amount of the desorbed ammonia was estimated.

2.4. Measurement scheme

In the adsorption experiments, the adsorbents were pretreated at $350\,^{\circ}C$ for 2 h to remove the organic contaminants and moisture prior to the experiments. In the first stage, fixed 200 mm bed length (around 2 g) was used to compare the toluene conversion with and without ozone in 2 h. In the second stage, a variable adsorbent bed length with ozone was used in order to achieve 90% toluene removal at different RH levels. The carrier gas for the adsorption experiments was supplied by the synthetic air containing 78% N_2 and 22% O_2. The RH and CO_2 levels were set to 0% in the first stage of the experiment in order to minimize the influence of these species on the catalytic activity. The inlet ozone level was fixed at 6 ppm (± 0.1 ppm) in the regular tests and 24 ppm (± 0.5 ppm) inlet ozone was also used in some cases to demonstrate the possibility of enhanced catalytic effects. The toluene level was maintained at 1.5 ppm (± 0.03 ppm) in the regular tests and a lower concentration level at 0.3 ppm (± 0.01 ppm) was also used in a few other cases to see the effect of lower toluene concentration. Temperature was regulated in the adsorption experiments in the range of 23–25 $^{\circ}C$. The flow rate was kept constant at $0.21\,m^3\,h^{-1}$, and thus the residence time in the adsorbent bed during the first stage experimental condition was around 0.13 s. The RH, CO_2, O_3 and toluene levels were recorded at 1 min interval. Each set of experiments lasted for 2 h and was repeated three times. Thermal desorption experiments at $350\,^{\circ}C$ were carried out after the adsorption experiments, with the same settings, but the carrier gas was N_2 at a flow rate of $0.18\,m^3\,h^{-1}$.

The toluene, CO_2 and O_3 levels were recorded, and the amount of the adsorbed species was estimated based on the time for the desorption process, mass concentration of each species and the supply flow rate.

3. Results and discussions

3.1. Material characterization

The adsorbents were identified as NaX, NaY and MCM-41 by PXRD analysis using the JCPDS database. The adsorbents were in powder form and the particle sizes of NaX and NaY were around 2 μm. The particle size of MCM-41 was around 0.1 μm. The phase purity and the crystal structure of the adsorbents were not damaged by 6 ppm ozone after three regeneration cycles. The BET surface area of NaX, NaY and MCM-41 was found to be 530, 592 and 975 $m^2 g^{-1}$. It was found that MCM-41 had the highest BET surface area with the 1-D hexagonal pore at 22.5 Å pore opening. NaY and NaX offered a similar BET surface area through the 3-D cage like pore with opening of 7.4 Å. The pore opening sizes and the BET surface areas of the adsorbents significantly influenced the selectivity and mass transfer resistance of molecule adsorption. The bulk chemical compositions of the adsorbents obtained by XRF analysis were shown in Table 1. The amount of Al in NaX was the highest indicating that the acid site density was the highest (Stöcker, 2005).

3.2. Acid strength and acid site density of the adsorbents

The NH_3-TGA analysis was conducted in order to compare the acid strength and acid site density of various adsorbents. The amount of ammonia desorbed in a given temperature range was taken as a measure of acid site density. The temperature range in which most ammonia was desorbed referred to the acid strength distribution. The results of the NH_3-TGA analysis were reported in Fig. 2 and the associated NH_3 desorption amount were presented in Table 2.

Throughout the desorption process (25–400 °C), around 1.7, 1.9 and 2.0 mg of NH_3 were desorbed from NaX, NaY and MCM-41 respectively. The NH_3 desorbed in the low temperature range (below 100 °C) was considered as physisorbed NH_3, and was not used for the determination of acid strength and acid site density. Around 0.4, 0.7 and 1.1 mg of NH_3 were desorbed from NaX, NaY and MCM-41 in the low temperature range, respectively. The total amount of chemisorbed NH_3 is proportional to the number of acid sites per unit mass of the adsorbents (acid site density). The total amount of NH_3 desorbed in the mid (100–190 °C) and high (190–400 °C) temperature ranges was defined as the chemisorbed NH_3 and was thus used as an indicator for the acid site density. On the other hand, the heat energy (temperature) required to release the NH_3 from the acid sites is proportional to the strength of the chemical bonds (acid strength) and hence the total amount of NH_3 desorbed in the high temperature range was used as an indicator for the acid strength.

In the mid-temperature range (100–190 °C), where the NaX and MCM-41 desorption curves met each other, around 1, 0.8 and 0.3 mg of the NH_3 were desorbed from the NaX, NaY and MCM-41, respectively. Most of the NH_3 (58.8%) in NaX was desorbed in this mid-temperature region and only 0.3 mg (18%) of the NH_3 from NaX was desorbed in the high temperature region (190–400 °C). In contrast, MCM-41 desorbed 0.6 mg of NH_3 in the high temperature range, which was about 30% of the total adsorbed NH_3. The data indicated the acid sites density in NaX was higher than that of NaY, followed by MCM-41. This was because 1.3 mg of NH_3 was chemisorbed in NaX in the mid- and high temperature ranges while only about 1.2 and 0.9 mg was chemisorbed in NaY and MCM-41. However, the MCM-41 demonstrated the highest acid strength as the amount of NH_3 desorbed in the high temperature region was larger than that of NaX and NaY. The NH_3-TGA profiles showed that the MCM-41 contained the lowest density of acid sites. This was consistent with its low Al content as shown in Table 1. However, it had a higher strength of acidity, which might compensate for the low acid density effect in its overall performance in pollutant removal.

Table 1
XRF analysis of NaX, NaY and MCM-41

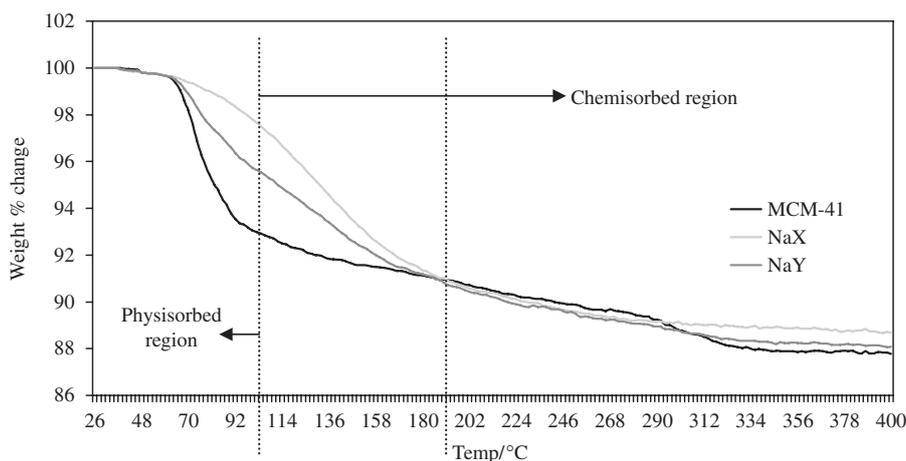| Element	Adsorbents		
	NaX	NaY	MCM-41
Na	12.8	11.6	1.6
Al	25.7	17.0	3.1
Si	53.5	68.4	94.1

Fig. 2. NH_3-TGA analysis of NaX, NaY and MCM-41.

Table 2
Amount of NH_3 desorbed (mg) for NH_3-TGA analysis

Temp. range (°C)	Adsorbents		
	NaX	NaY	MCM-41
25–100 (low)	0.4 (24%)	0.7 (36%)	1.1 (55%)
100–190 (mid)	1.0 (58%)	0.8 (41%)	0.3 (15%)
190–400 (high)	0.3 (18%)	0.4 (23%)	0.6 (30%)
Total	1.7 (100%)	1.9 (100%)	2.0 (100%)

3.3. Removal of toluene without ozone

The effect of different adsorbents (NaX, NaY and MCM-41) on toluene adsorption without the use of ozone was plotted in Fig. 3. During the adsorption tests (1.5 ppm toluene, 0% relative humidity, 0% CO_2 concentration, 200 mm adsorbent bed length and without the use of ozone), MCM-41 performed the best. Around 73% of the toluene was removed, while 53% and 45% of the toluene were removed by NaY and NaX. The MCM-41, NaY and NaX adsorbed 1.75, 1.25 and 1.07 mg of toluene, respectively. Such a difference may be attributed to the high BET surface area and the large accessible internal pore volume of MCM-41 compared to NaY and NaX.

3.4. Removal of toluene with ozone

Fig. 3 also presents the results when 6 ppm ozone was used over MCM-41, NaY and NaX. MCM-41 had the capacity to reduce the toluene level from 1.5 ppm at inlet to around 0.2 ppm at outlet.

Approximately 2.16 mg (90%) of toluene was removed within a 200 mm bed length. The toluene removal performance of NaY and NaX were also enhanced by the use of ozone, with the exit toluene levels down to about 0.3 and 0.5 ppm, respectively. Around 1.85 and 1.70 mg of the toluene were removed by the NaY and NaX, respectively. Based on the experimental results, MCM-41 offered the best toluene removal performance when using ozone, since the adsorption capacity of MCM-41 for toluene was the highest as discussed in the previous section. In addition, the acid strength of MCM-41 was also the strongest from the NH_3-TGA results, so it could effectively convert ozone into atomic oxygen for the subsequent reactions with toluene. The residual ozone level from MCM-41 was about 95 ppb. Over 98% of the inlet ozone was consumed. H_2O and CO_2 were not detected in the effluent indicating that they were captured by the adsorbents. This could have an impact on the saturation of catalytic reaction sites during long operation, leading to gradual deterioration of performance.

Even though the acid strengths of zeolite NaX and NaY were not as strong as MCM-41, the acid site densities of NaY and NaX were high enough to decompose ozone into atomic oxygen for the reaction with toluene. As a result, it was seen that the toluene removal performances with the use of ozone were also significantly improved. From Fig. 3, the removal performance increased from 52.5% to 78.0% for NaY while the removal of toluene over NaX was enhanced from 45% to 71.6%. The residual ozone from NaY and NaX was higher than that of MCM-41, about 538 and 770 ppb, respectively. The significantly lower
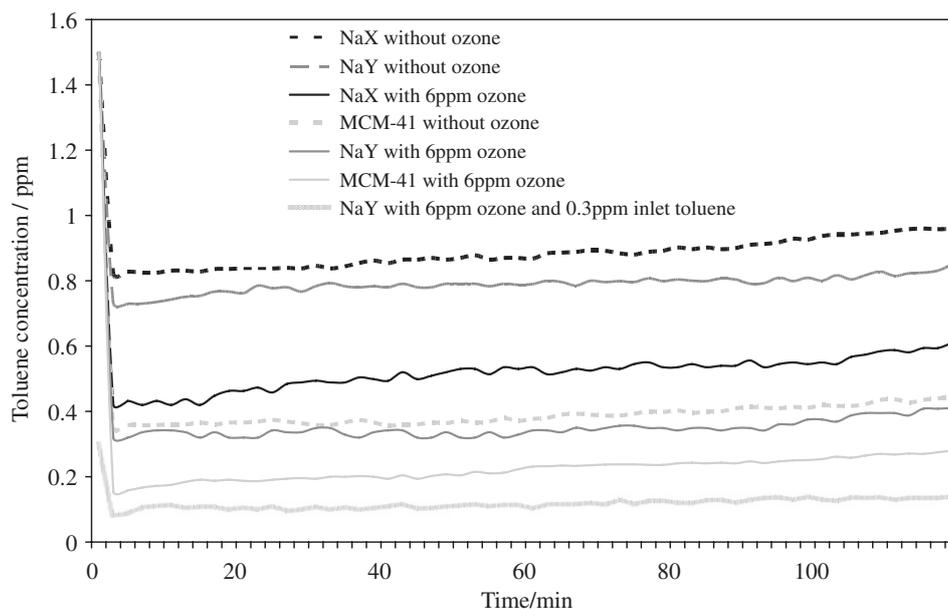
Fig. 3. Downstream toluene concentration with 200 mm bed length over various adsorbents with and without ozone.

residual ozone level in MCM-41 was perhaps due to the higher mass transfer rate of ozone per unit weight of adsorbent in MCM-41 compared to NaY and NaX, as the BET surface area of MCM-41 was the highest. The CO_2 and H_2O level in the effluent were below detection limits.

The challenge of the ozonation effect at a lower pollutant concentration was taken with toluene inlet level at 0.3 and 6 ppm ozone over NaY. The results were also plotted in Fig. 3. It was seen that the toluene level reduced to around 0.1 ppm with the ozonation effects. The removal efficiency improved from 40% without ozone to around 70% with the use of 6 ppm ozone and the residual ozone was about 920 ppb. The residual ozone was moving to a higher level as the absolute amount of the ozone involved in the reaction decreased. Besides, the overall removal efficiency at the lower toluene concentration was lower than that at 1.5 ppm probably owing to the adsorption isotherm of the adsorbent.

3.5. Bed length required to achieve 90% toluene conversion efficiency with minimum residual ozone

In order to minimize residual ozone levels and achieve 90% toluene conversion efficiency, various adsorbent bed lengths were tried. Table 3 compares the bed length for NaX, NaY and MCM-41 to achieve 90% toluene conversion at 0% RH and 50% RH. The corresponding residence time was

Table 3
Bed length required to remove 90% toluene at 6 ppm ozone over various adsorbents and RH levels

Adsorbents	Bed length required (mm)/residence time (s)	
	RH level	
	0%	50%
NaX (0 ppm ozone)	450/0.29	>450/>0.29
NaX	350/0.23	420/0.28
NaY	230/0.15	240/0.16
MCM-41	200/0.13	230/0.15

also shown in the table. It seemed that ozone shortened the bed length substantially as the NaX bed length decreased from 450 to 350 mm.

In dry conditions with 6 ppm ozone, MCM-41 required the shortest bed length (200 mm) to achieve 90% toluene removal, followed by NaY (230 mm) and NaX (350 mm). The residual ozone levels were lower than 130 ppb in all cases, close to the upper exposure limits by NIOSH (2007). This trend followed the order of the adsorption performance in Fig. 3 and the surface area from BET analysis. The catalytic effects of the adsorbents on toluene were similar, as reported previously. However, the large pore opening and high BET surface area of MCM-41 reduced the mass transfer resistance of ozone and toluene. These enhanced the overall

performance and explained why lower amount of MCM-41 was required.

The adsorbent performance in a humid environment (50% RH) was also shown in Table 3. Again, least amount of MCM-41 was required to achieve the target. However, the use of the adsorbents in humid environment to achieve the same target was higher compared with dry conditions. An additional quantity of 20% and 15% of NaX and MCM-41 was required because NaX and MCM-41 adsorbs moisture, which competes with ozone and toluene for reaction sites. However, less than 5% additional NaY was required to achieve the goal in a humid environment as NaY was hydrophobic.

3.6. Thermal desorption of toluene, O_3, CO_2 and other intermediate species from the adsorbents

The thermal desorption experiments of toluene, ozone, CO_2 and intermediate species from the adsorbents were conducted after the adsorption experiments. Catalytic activity can roughly be estimated by using the information from the thermal desorption experiment. Table 4a–c showed the thermal desorption data of the adsorbents after the 2 h experiments involving 1.5 ppm toluene and 6 ppm ozone in 200 mm bed. The amount of consumption referred to the difference between the inlet and outlet species content, while the reacted amount in the last column referred to the difference between the consumed amount and the desorption amount quantified from the desorption tests. Throughout the desorption process, around 1.31, 1.38 and 1.72 mg of toluene was desorbed from NaX, NaY and MCM-41, respectively. The thermal desorption data were consistent with the adsorption experiments in which the toluene handling capability of MCM-41 was the highest.

Our previous study (Chao et al., 2007) proposed that O_3 was decomposed into O_2 and active atomic O* at the Lewis acid sites based on the ozone decomposition mechanisms in MgO (Einaga and

Table 4

NaX	Supply (mg)	Consumption (mg)	Desorption (mg)	Reacted (mg)
(a) NaX adsorption–desorption data				
Test with 6 ppm ozone and 1.5 ppm toluene				
Toluene	2.38	1.70	1.31	0.39
Ozone	4.96	4.32	0	4.32
CO_2	0	0	1.02	1.02
NaY	**Supply (mg)**	**Consumption (mg)**	**Desorption (mg)**	**Reacted (mg)**
(b) NaY adsorption-desorption data at 1.5 and 0.3 ppm toluene with 6 ppm ozone				
Test with 6 ppm ozone and 1.5 ppm toluene				
Toluene	2.38	1.85	1.38	0.47
Ozone	4.96	4.52	0	4.52
CO_2	0	0	1.22	1.22
Test with 6 ppm ozone and 0.3 ppm toluene				
Toluene	0.48	0.35	0.22	0.13
Ozone	4.96	4.14	0	4.14
CO_2	0	0	0.39	0.39
MCM-41	**Supply (mg)**	**Consumption (mg)**	**Desorption (mg)**	**Reacted (mg)**
(c) MCM-41 adsorption-desorption data with 6 and 24 ppm ozone				
Test with 6 ppm ozone and 1.5 ppm toluene				
Toluene	2.38	2.16	1.72	0.44
Ozone	4.96	4.88	0	4.88
CO_2	0	0	1.39	1.39
Test with 24 ppm ozone and 1.5 ppm toluene				
Toluene	2.38	2.29	1.36	0.93
Ozone	20.00	16.18	0	16.18
CO_2	0	0	2.89	2.89

Futamura, 2004; Li et al., 1998):

$$O_3 + s \rightarrow sO_3, \tag{1}$$

$$sO_3 \rightarrow sO^* + O_2, \tag{2}$$

where "s" and "sO_3" denote the Lewis acid site in the adsorbents and the O_3 attached to the Lewis acid site, respectively. If toluene (C_7H_8) is present, it reacts with the active atomic O^* following the overall reaction equation when complete reaction can be attained:

$$C_7H_8 + 18O^* \rightarrow 7CO_2 + 4H_2O. \tag{3}$$
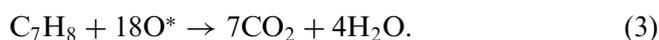
O_2 is one of the major ozone decomposition products from Eq. (2) (Roscoe and Abbatt, 2005). CO_2 and H_2O are the complete reaction products from Eq. (3). In practice, incomplete reaction occurs generating intermediate species.

Several other possible mechanisms were proposed for the catalytic ozonation of VOCs. The first possible mechanism is that both toluene and ozone are adsorbed into the adsorbent. The adsorbed ozone could undergo a decomposition process and is converted into OH radicals for subsequent VOC reactions (Kastner et al., 2005). However, the OH radical formation requires water. In this study, the removal efficiency of toluene decreased with the moisture content in the supply air and the system performed better in dry condition. This showed the OH radical might not be converted in the ozone decomposition process and hence the OH radical might not play a critical role. The other possible mechanism is that the adsorbed VOCs on the adsorbent react directly with the gas-phase ozone. The reaction rate of the VOCs depends on the gas-phase ozone concentration. The typical example with this mechanism is the catalytic ozonation of alcohol over SiO_2 (Oyama, 2000; Kastner et al., 2005). SiO_2 has a high alcohol but low ozone adsorption capacity. On the contrary, the adsorbent used in this study demonstrated good adsorption capacity for both toluene and ozone. As a result, the removal of toluene due to this mechanism is believed to be minimal as the toluene removal with ozone over the toluene-saturated sample was weak compared with the unsaturated samples.

The data from desorption experiments can be used as an indicator of the catalytic activity. The CO_2 desorption data from NaX, NaY and MCM-41 was found to be 1.02, 1.22 and 1.39 mg, respectively. The adsorption/reaction ratio of toluene was also estimated. For example, the NaX consumed 1.7 mg

toluene and 1.31 mg was desorbed. The reacted toluene was around 0.39 mg which was about 23% of the total toluene removed in the NaX/Ozone system. Similar ratios of 25% and 20% were obtained for NaY and MCM-41, respectively. Table 5 showed the number of moles of reacted toluene, reacted ozone and generated CO_2, based on data from the adsorption and desorption experiments. The amounts of toluene that reacted with ozone were comparable. This seemed to indicate the extent of catalytic activity among the adsorbents was similar. Although the acid strength in MCM-41 was stronger than that of NaY and NaX, the low acid density seemed to offset the overall catalytic performance.

The toluene/ozone stoichiometric ratio was 1:18 from Eq. (3) and the experimental ratio of NaX, NaY and MCM-41 were $9/0.43 = 20.9$, $9.4/0.51 = 18.4$ and $10/0.48 = 20.8$, respectively. The experimental ratios were higher showing that actual ozone consumption was higher. The CO_2 to toluene ratios corresponding to the different adsorbents were also investigated. It was found that the experimental ratios were close to, but generally lower than stoichiometric ratio (7:1). The actual CO_2 to toluene ratios were around 5.4:1, 5.4:1 and 6.6:1 for NaX, NaY and MCM-41, respectively. Some O atoms from the ozone decomposition did not react with toluene to form CO_2 and H_2O, but might be converted into O_2 during the regeneration process at the acid sites (Roscoe and Abbatt, 2005). This competitive effect in the formation of oxygen made the deviations from the stoichiometric ratios.

Enhancement of the ozonation effects can be done by varying the inlet ozone level or applying supplementary treatment on the adsorbents. The catalytic ozonation effect of toluene could be enhanced by modifying the inlet toluene to ozone ratios. In the cases of using lower toluene level at 0.3 ppm over NaY as shown in Table 4b, the catalytic effect was enhanced to around 37% with excessive supply of ozone for the reactions.

Table 5
Number of mole of toluene, ozone and CO_2 desorbed

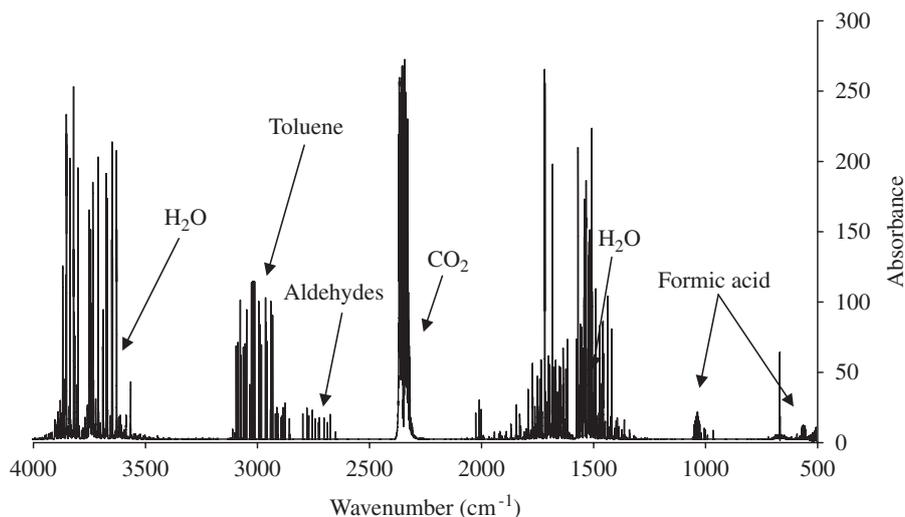|	Toluene reacted with ozone (mol $\times 10^{-5}$)	Ozone reacted (mol $\times 10^{-5}$)	CO_2 generated (mol $\times 10^{-5}$)
NaX	0.43	9	2.32
NaY	0.51	9.4	2.77
MCM-41	0.48	10	3.17

Fig. 4. Outlet gas spectrum of MCM-41 during the thermal desorption experiment.

The other case that enhanced the catalytic effects was shown in Table 4c with 24 ppm inlet ozone in the MCM-41 adsorption system. Around 40% of the toluene was removed via catalytic ozonation and the overall removal efficiency was elevated to above 96%. However, its residual ozone level with 200 mm bed length may not be desirable for indoor application and thus the extension of the bed length for extra ozone decomposition is required. Alternatively, an after-treatment ozone decomposition catalyst may be used to diminish the residual ozone (Oyama, 2000). The other way to enhance the catalytic activity is to use the adsorbents containing transition metals. Our previous study showed that the catalytic effect on the removal of acetone at room temperature was enhanced over cobalt exchanged NaX compared with the parent form adsorbents (Law et al., 2003). Nevertheless, this study aimed to investigate the basic reaction mechanism involving toluene, ozone and various kinds of adsorbents and hence the ozonation effect over the adsorbents containing transition metals was not studied at the current stage which could be a good direction for future work.

The intermediate species in the desorption gas stream were identified by the gas phase FT-IR and the corresponding spectrum for MCM-41 was shown in Fig. 4. Apart from toluene and CO_2, trace amounts of gas phase aldehydes and formic acids (CH_2O_2) were identified. The aldehyde species could be formaldehyde (HCHO), acetaldehyde (CH_3CHO) and benzaldhyde (C_6H_5CHO). Their concentrations were much lower than toluene and CO_2 as seen in Fig. 4. These intermediates probably

came from the incomplete breakdown of toluene by the atomic oxygen as the number of carbon in the intermediates was lower than that in the toluene molecules. These intermediates were only found in the thermal desorption gas stream but they were not detected in the exhaust gas stream during the adsorption experiments. Most of the intermediates were adsorbed in the adsorbents and this is an added advantage over the other air purification technologies as most of the intermediates were not released in the gas stream during the operations. However, the pressure drop across the adsorbent bed may be one of the potential challenges. Another challenge is that the performance of the ozonation system could vary with individual VOC compounds. One set of our unpublished data showed that methane was inert in the ozonation system at room temperature unless the temperature was increased. Using a different VOCs apart from toluene may lead to a reaction mechanism different from the one proposed above. A mixture of different VOCs will lead to competitive effect among different species. Detailed investigations on various single VOC compounds and the mixture of VOCs over the ozonation system are required to further implement the use of this purification technology.

4. Conclusions

Catalytic oxidization of toluene by ozone over NaX, NaY and MCM-41 was studied experimentally. Toluene conversion was enhanced when ozone was injected. MCM-41 performed best in the dry conditions, followed by NaY and NaX.

The catalytic effects on 1.5 ppm toluene over the adsorbents were around 20–25% while the rest, around 70%, were by adsorption. This indicated that the catalytic effect by the acid strength may be offset by the acid site density of the adsorbents and vice versa. The overall conversion efficiency and residual ozone concentration can further be optimized by adjusting the toluene/ozone ratio or extending the adsorbent bed length. Intermediates such as aldehydes and organic acid were only identified in the desorbed gas indicating that those species were retained in the adsorbents. The performance of the hydrophilic zeolite NaX was significantly affected by the moisture content, whereas the performance of NaY and MCM-41 were relatively stable in the humid environment. The removal characteristics of various adsorbents suggested that ozonation of toluene over MCM-41 may be applicable for indoor applications since the overall removal efficiency is high with minimum residual ozone. On the other hand, reasonable performances were demonstrated by NaX and NaY. They may be suitable for industrial applications as the residual ozone could meet the industrial standards with potentially cheaper material costs. However, the catalytic performance may be different with other VOCs under the same experimental conditions and thus more extensive evaluation is needed to validate the effects.

Acknowledgement

References

Boeniger, M., 1995. Use of ozone generating devices to improve indoor air quality. American Industrial Hygiene Association Journal 56, 590–598.

Chandak, M.V., Lin, Y.S., 1998. Hydrophobic zeolites as adsorbents for removal of volatile organic compounds from air. Environmental Technology 19, 941–948.

Chao, C.Y.H., Kwong, C.W., Hui, K.S., 2007. Potential use of a combined ozone and zeolite system for gaseous toluene elimination. Journal of Hazardous Materials 143 (1–2), 118–127.

Chen, W., Zhang, J.S., Zhang, Z., 2005. Performance of air cleaners for removing multiple volatile organic compounds in indoor air. ASHRAE Transactions 111, 1101–1114.

Delage, F., Pre, P., Cloirec, P.L., 2000. Mass transfer and warming during adsorption of high concentrations of VOCs on an activated carbon bed: experimental and theoretical analysis. Environmental Science & Technology 34, 4816–4821.

Einaga, H., Futamura, S., 2004. Catalytic oxidation of benzene with ozone over alumina-supported manganese oxides. Journal of Catalysis 227, 304–312.

Hodgson, A.T., Destaillats, H., Sullivan, D.P., Fisk, W.J., 2007. Performance of ultraviolet photocatalytic oxidation for indoor air cleaning applications. Indoor Air 17 (4), 305–316.

Hui, K.S., Chao, C.Y.H., 2006. Synthesis of MCM-41 from coal fly ash by a green approach: Influence of synthesis pH. Journal of Hazardous Materials 137 (2), 1135–1148.

Kastner, J.R., Buquoi, Q., Ganagavaram, R., Das, K.C., 2005. Catalytic ozonation of gaseous reduced sulfur compounds using wood fly ash. Environmental Science & Technology 39, 1835–1842.

Law, T.S.C., Chao, C.Y.H., Chan, G.Y.W., Law, A.K.Y., 2003. Confined catalytic oxidation of volatile organic compounds by transition metal containing zeolite and ionizer. Atmospheric Environment 37 (38), 5433–5437.

Law, T.S.C., Chao, C.Y.H., Chan, G.Y.W., Law, A.K.Y., 2004. The use of zeolite and oxidant generating devices in air cleaning. Indoor and Built Environment 13, 45–51.

Li, W., Gibbs, G.V., Oyama, S.T., 1998. Mechanism of ozone decomposition on a manganese oxide catalyst. 1. In situ Raman spectroscopy and ab initio molecular orbital calculations. Journal of the American Chemical Society 120, 9041–9046.

NIOSH. Pocket guide to chemical hazard. See ⟨http://www.cdc.gov/niosh/npg/npgd0476.html⟩ (accessed November 2007).

Niu, J.L., Tung, T.C.W., Burnett, J., 2001. Ozone emission rate testing and ranking method using environmental chamber. Atmospheric Environment 35 (12), 2143–2151.

OSHA. Occupational safety and health guideline for toluene. See ⟨http://www.osha.gov/SLTC/healthguidelines/toluene/recognition.html⟩ (accessed November 2007).

Oyama, S.T., 2000. Chemical and catalytic properties of ozone. Catalysis Reviews—Science and Engineering 42, 279–322.

Roscoe, J.M., Abbatt, J.P.D., 2005. Diffuse reflectance FTIR study of the interaction of alumina surfaces with ozone and water vapour. Journal of Physical Chemistry 109, 9028–9034.

Ryoo, R., Jun, S., Kim, J.M., Kim, M.J., 1997. Generalised route to the preparation of mesoporous metallosilicates via post-synthetic metal implantation. Chemical Communications, 2225–2226.

Stöcker, M., 2005. Gas phase catalysis by zeolites. Microporous and Mesoporous Materials 82, 257–292.

Sæbjörnsson, K.O., Fang, L., 2006. Laboratory study on incomplete oxidation of a photocatalytic oxidation air purifier. In: Proceedings of Healthy Buildings 2006, pp. 271–276.

USEPA. Ozone generators that are sold as air cleaners. See ⟨http://www.epa.gov/iaq/pubs/ozonegen.html⟩ (accessed November 2007).

Weschler, C.J., 2000. Ozone in indoor environments: concentration and chemistry. Indoor Air 10, 269–288.

Yang, R., Zhang, Y.P., Xu, Q.J., Mo, J.H., 2007. A mass transfer based method for measuring the reaction coefficients of a photocatalyst. Atmospheric Environment 41 (6), 1221–1229.

Yu, K.P., Lee, G.W.M., Hsieh, C.P., Yang, S.H., 2005. Using ozone air cleaners to remove indoor volatile organic compounds. In: Proceedings of the 10th International

Conference on Indoor Air Quality, Indoor Air 2005, Beijing, China, pp. 2981–2985.

Yu, K.P., Lee, G.W.M., Huang, W.M., Wu, C., Yang, S., 2006. The correlation between photocatalytic oxidation performance and chemical/physical properties of indoor volatile organic compounds. Atmospheric Environment 40 (2), 375–385.

Zhang, Y.P., Yang, R., Zhao, R.Y., 2003. A model for analyzing the performance of photocatalytic air cleaner in removing volatile organic compounds. Atmospheric Environment 37 (24), 3395–3399.

Zhao, X.S., Ma, Q., Lu, G.Q.M., 1998. VOC removal: comparison of MCM-41 with hydrophobic zeolites and activated carbon. Energy and Fuels 12, 1051–1054.